



Tumor Stabilization Induced by T-Cell Recruitment Fluctuations

Irina Bashkirtseva and Lev Ryashko
*Institute of Mathematics and Computer Sciences,
Ural Federal University, 620000, Lenina, 51,
Ekaterinburg, Russia*

Álvaro G. López, Jesús M. Seoane and Miguel A. F. Sanjuán
*Nonlinear Dynamics, Chaos and Complex Systems Group,
Departamento de Física, Universidad Rey Juan Carlos,
Tulipán s/n, 28933 Móstoles, Madrid, Spain*

Received January 24, 2020

The influence of random fluctuations on the recruitment of effector cells towards a tumor is studied by means of a stochastic mathematical model. Aggressively growing tumors are confronted against varying intensities of the cell-mediated immune response for which chaotic and periodic oscillations coexist together with stable tumor dynamics. A thorough parametric analysis of the noise-induced transition from this oscillatory regime to complete tumor dominance is carried out. A hysteresis phenomenon is uncovered, which stabilizes the tumor at its carrying capacity and drives the healthy and the immune cell populations to their extinction. Furthermore, it is shown that near a crisis bifurcation, such transitions occur under weak noise intensities. Finally, the corresponding noise-induced chaos-order transformation is analyzed and discussed in detail.

Keywords: Bifurcation analysis; nonlinear systems; mathematical modeling; cancer dynamics; fluctuations.

1. Introduction

It has been recently shown that tumor-immune interactions can display transient and permanent chaotic dynamics [Itik & Banks, 2010; López *et al.*, 2014a]. As discussed in those works, such dynamical scenarios are relevant when therapies are considered, due to the resurgence of residual tumor cells that might survive the treatment. The problem of tumor recurrence is specially important in the context of immunotherapy [Lasinska *et al.*, 2019], since it is related to the phenomenon of tumor dormancy [López *et al.*, 2017b]. Generally speaking, the immune system can be regarded as a control system that coevolves with a tumor mass acting as a natural selective force. Besides, it edits its phenotype by selecting those cells that are unresponsive

to immune detection [Aguirre-Ghiso, 2007; Teng *et al.*, 2008; Dunn *et al.*, 2004]. As demonstrated in previous studies [López *et al.*, 2017b], the levels of T-cell recruitment play a key role in the maintenance of tumor cell populations at low levels. The recruitment of effector cells is a very complicated process, since it involves many different types of cells and molecules. The extravasation of leukocytes requires an initial contact between such cells and the adjacent endothelial cells, which depends on different adhesion molecules. Once the cells adhere to the walls of the vessels, the immune cells traverse them through diapedesis, which again relies on several cytokines. Finally, chemokines bias their random walks to the tumor site [Janeway *et al.*, 2012; Miller *et al.*, 2003].

Mathematical models of tumor growth and its interaction with the immune system have demonstrated their potential to explain different properties of tumor-immune interactions [Bellomo & Preziosi, 2000; Wodarz & Komarova, 2014; Bellomo *et al.*, 2008]. More specifically, a two-dimensional ordinary differential equation model describing the coevolution of tumors in the presence of an immune response was originally presented by Kuznetsov *et al.* [1994]. This seminal model and their evolved variants have been extensively studied from the point of view of phase space analysis and the theory of bifurcations [De Pillis & Radunskaya, 2003; De Pillis *et al.*, 2005; De Pillis *et al.*, 2006; López *et al.*, 2014b; Nani & Freedman, 2000].

Due to a strong nonlinearity, models of tumor-immune interaction frequently exhibit multistability with the coexistence of regular and chaotic regimes. It is well known that a presence of inevitable random disturbances in nonlinear systems can result in crucial changes in the dynamical behavior and cause various phenomena, e.g. the stochastic resonance [McDonnell *et al.*, 2008], noise-induced transitions [Horsthemke & Lefever, 1984; Anishchenko *et al.*, 2007; Bashkirtseva *et al.*, 2018], stochastic excitement [Lindner *et al.*, 2004; Ryashko & Slepukhina, 2017] and noise-induced chaos [Gao *et al.*, 1999]. Stochastic effects in tumor-immune systems have received much attention in the past few years (see, e.g. [Fiasconaro *et al.*, 2006; Caravagna *et al.*, 2010; Liu *et al.*, 2018; Li & Zhao, 2019; Yang *et al.*, 2019] and bibliography therein). But even in the deterministic case, not much research has been oriented towards the importance of the levels of the T-cell recruitment [López *et al.*, 2017b] and, as far as the authors are concerned, none has evaluated in detail the effects of modifying the parameter that simulates this phenomenon. Furthermore, the specific nature of this function varies among different studies [Kuznetsov *et al.*, 1994; De Pillis *et al.*, 2005] with little justification. Contrary to the process of tumor cell lysis, which has been more deeply studied from the mathematical point of view, the function describing the rate of T-cell recruitment to the tumor site clearly deserves more attention. As previously commented, this process is of tremendous complexity and great variations among different types of tumors are expected, depending on the tissue location and other factors, as for instance the degree of inflammation. Moreover, even within a particular

tumor that evolves under the dynamical influence of the adaptive immune response, high fluctuations of this parameter must occur as time goes by.

In the present work, we study the influence of parametric perturbations of the T-cell recruitment in dynamical system that contains three ordinary differential equations. After introducing the unperturbed dynamical system in Sec. 2 and investigating the bifurcation phenomena therein, we write down the Langevin equations using multiplicative white Gaussian noise in Sec. 3. We then proceed to present our main results and characterize the different types of dynamical transitions observed in the probabilistic model using standard tools from the theory of stochastic processes. Then, in Sec. 4, we delve deeper into the noise-induced transition from the chaotic regime to the globally stable regime. As usual, the closing section is devoted to expose the most resounding findings and possible future research concerning the mathematical modeling of tumor and immune cell recruitment in the present context.

2. Deterministic Mathematical Model

We begin by considering a dynamical model of tumor-immune cell interactions, whose dynamical equations read

$$\begin{aligned}\dot{T} &= r_1 T \left(1 - \frac{T}{k_1}\right) - a_{12} TH - a_{13} TE \\ \dot{H} &= r_2 H \left(1 - \frac{H}{k_2}\right) - a_{21} HT \\ \dot{E} &= r_3 \frac{ET}{T + k_3} - a_{31} ET - d_3 E,\end{aligned}\tag{1}$$

where the variable $T(t)$ represents the tumor cells, $H(t)$ describes the healthy host cells that form the tissue where the tumor has emerged and $E(t)$ stands for the effector immune cells (e.g. cytotoxic CD8+T lymphocytes). This competition Lotka-Volterra based model is essentially the same as another model originally presented in previous works [De Pillis & Radunskaya, 2003] to study optimal schedules in cancer chemotherapy, and we refer the reader to such references for a more detailed description. All the biological assumptions considered to develop the model equations are based on both accepted knowledge of basic laws governing tumor growth and the immune system function

[Kuznetsov *et al.*, 1994]. Moreover, we recall that some versions of the present model have been tested against *in vivo* experimental data [De Pillis *et al.*, 2006; López *et al.*, 2014b]. The cancer and the healthy cells exhibit limited growth represented by two respective logistic functions, with similar rates of growth r_1 and r_2 , and carrying capacities K_1 and K_2 [López *et al.*, 2014b]. It is also considered that tumor and healthy cells compete for space and resources, where the rates of competition are given by the parameters a_{12} and a_{21} . Concerning the immune cells, it is assumed that cytokine emission triggers the adaptive immune response producing the recruitment of cytotoxic T-cells to the tumor domain at a maximum constant rate r_3 . This phenomenon is considered to act without time-delay and it is approximated by a Michaelis–Menten functional response, where k_3 represents the number of tumor cells for which the rate of recruitment is half of its maximum. Again, two Lotka–Volterra competition terms, with rates a_{13} and a_{31} , have been assumed between tumor and immune cells, since the former find ways to counterattack the latter [López *et al.*, 2014b]. Finally, after several encounters (or in the absence of competitors), the effector cells inactivate (or die off) at a constant per capita rate d_3 .

A nondimensionalized model can be readily derived, yielding the simplified equations

$$\begin{aligned} \dot{x} &= x(1 - x) - a_{12}xy - a_{13}xz \\ \dot{y} &= r_2y(1 - y) - a_{21}xy \\ \dot{z} &= r_3 \frac{x}{x + k_3} z - a_{31}xz - d_3z, \end{aligned} \tag{2}$$

where $x(t)$, $y(t)$ and $z(t)$ are densities of populations of tumor cells, healthy host cells, and effector immune cells, respectively. In other works only equilibrium regimes were covered [De Pillis & Radunskaya, 2003]. On the other hand, the constant input of immune cells into the tissue can be eliminated, disregarding the innate immune response [Itik & Banks, 2010]. Parametric zones with regular and chaotic oscillatory dynamics were discovered and extensively described from a mathematical point of view. Later on, a new parametric zone, closer to the original set of parameters was found, with coexisting chaotic and equilibrium attractors near a boundary crisis [López *et al.*, 2014a]. Here we follow this last reference and fix the parameter values as

$$\begin{aligned} a_{12} &= 0.5, & a_{21} &= 4.8, & a_{13} &= 1.2, & a_{31} &= 1.1, \\ r_2 &= 1.2, & d_3 &= 0.1, & k_3 &= 0.3 \end{aligned}$$

in order to study the system dynamics under the variation of the parameter r_3 . This parameter is relevant in our work since it characterizes the rate of immune cell recruitment as a consequence of their interaction with the tumor cells and subsequent cytokine emission. As a reminder, the parameters of this model are reasonable from an empirical point of view [López *et al.*, 2014b]. Two different parameters in comparison with the original set of values correspond to r_3 and a_{21} , which take higher values. This set of values corresponds to very immunogenic and aggressively competing tumors (e.g. acidification is high).

As we have previously indicated, the parameter r_3 plays a key role in the present study [López *et al.*, 2017a]. Small changes of r_3 can result in catastrophic shifts, even for the deterministic dynamical system appearing in Eqs. (2). These shifts can be explained mathematically by corresponding bifurcations. In this study, we will consider $r_3 \in [1.25, 1.65]$. In this range of parameters, the dynamical system presents five or six fixed points in the positive octant as shown in the 3D phase space depicted in Fig. 1. For our numerical simulations, we take the value $r_3 = 1.291$, again according to a previous work [López *et al.*, 2014a]. Using this parameter value the origin $O(0, 0, 0)$ is a saddle fixed point. It has two positive eigenvalues aligned with the x

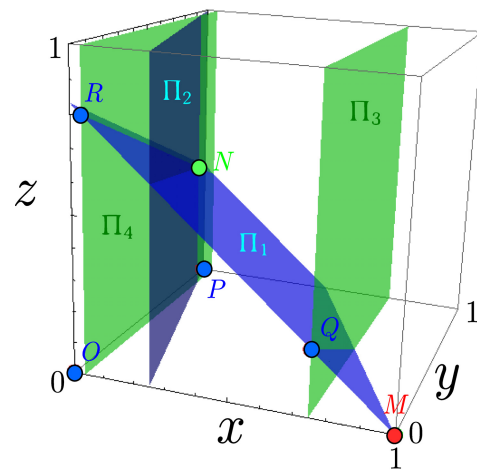


Fig. 1. General view of the phase space. The deterministic model represented in Eqs. (2) presents six fixed points, which are the result of different intersecting planes. In addition to the x , y and z planes (not colored), we can see four more nullclines Π_i , with $i = 1, \dots, 4$. The equilibrium representing the malignant state M is represented in red color, while another fixed point N taking place for small tumor size populations is plotted in green. Chaotic and periodic oscillations organize around this unstable spiral.

and y axes, while a third negative eigenvalue is associated to the remaining z -axis. The point $P(0, 1, 0)$ represents the tumor-free solution, for which only normal cells can be found. As long as we keep in the plane $x = 0$, this fixed point is stable. On the contrary, the point $M(1, 0, 0)$ represents the stable solution for which only tumor cells can be found. Therefore, this third fixed point represents a dangerous malignant attractor. Indeed, for this equilibrium the eigenvalues of the Jacobian matrix are

$$\lambda_1 = -1, \quad \lambda_2 = r_2 - a_{21} = -3.6,$$

$$\lambda_3 = \frac{r_3}{1 + k_3} - a_{31} - d_3.$$

This equilibrium is always stable in the plane $z = 0$. In the 3D phase space, this equilibrium is stable for $r_3 < r_3^* = (a_{31} + d_3)(1 + k_3) = 1.56$. Thus, if the recruitment of the T-cells is high enough, the malignant state loses its stability. The saddle

fixed point $Q(0.75, 0, 0.21)$ has a two-dimensional stable manifold that separates the basins of attraction of the malignant tumor fixed point and the chaotically oscillating attractor. Two spiral-saddles $R(0.04, 0, 0.8)$ and $N(0.04, 0.85, 0.45)$ remain. The former R spirals stably, with its unstable direction pointing closely to the direction of the y -axis. The latter displays inverted stability, i.e. it is the spiral that is unstable. These two confronted spiral-saddles ceaselessly interchange their dynamics leading to the heteroclinic chaotic (or periodic) behavior of this dynamical system (see Fig. 2). The nondegenerate equilibrium $N(\bar{x}, \bar{y}, \bar{z})$ has positive coordinates

$$\bar{x} = \frac{r_3 - a_{31}k_3 - d_3 - \sqrt{(r_3 - a_{31}k_3 - d_3)^2 - 4a_{31}d_3k_3}}{2a_{31}},$$

$$\bar{y} = 1 - \frac{a_{21}\bar{x}}{r_2}, \quad \bar{z} = \frac{1 - \bar{x} - a_{12}\bar{y}}{a_{13}}.$$

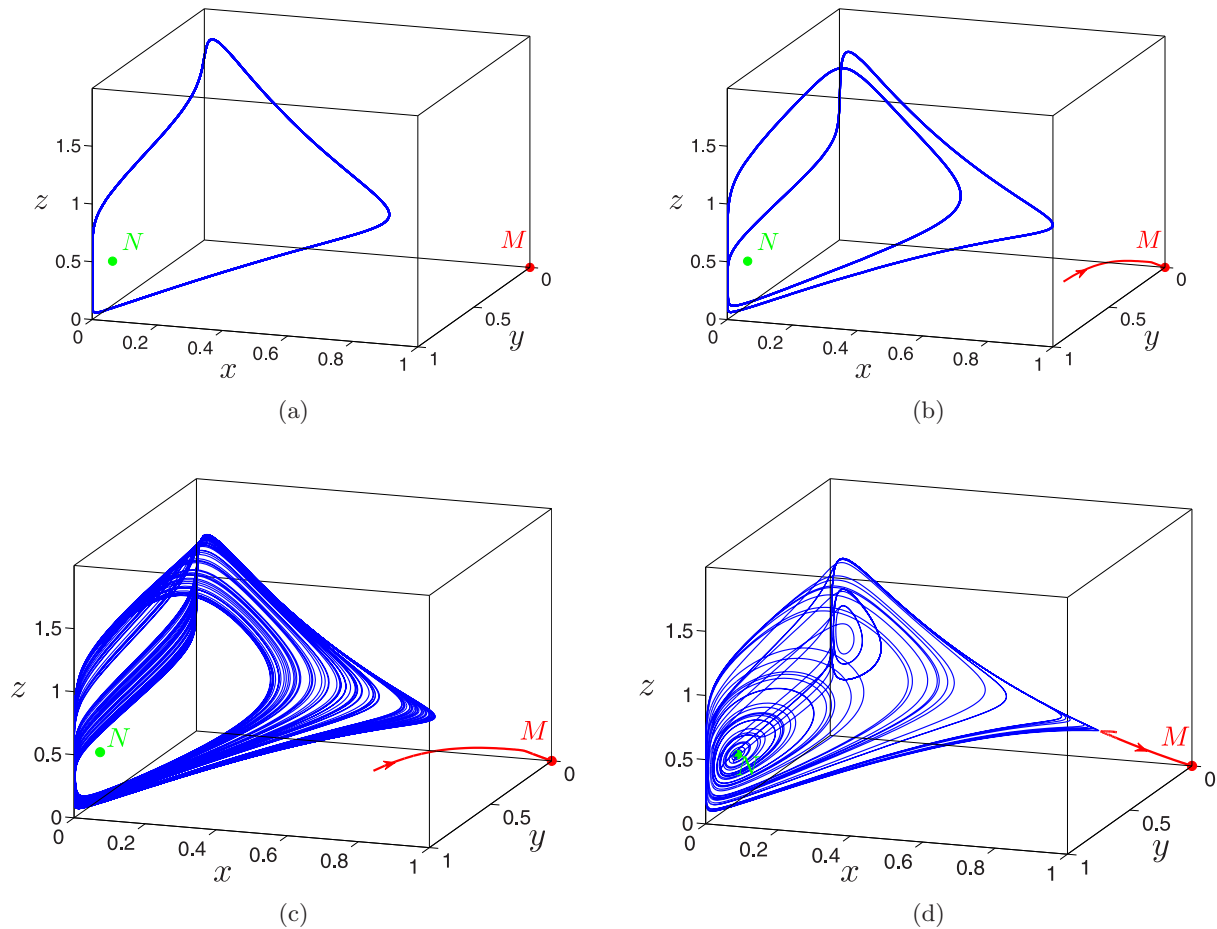


Fig. 2. Regular and chaotic oscillatory attractors. The phase space trajectories of the model appearing in Eqs. (2) are represented. A saddle fixed point N and a malignant attractor M appear in green and red colors, respectively. (a) A periodic cycle is found for $r_3 = 1.6$. (b) A two period trajectory appears for $r_3 = 1.5$. (c) A chaotic attractor formed by two bands is found for $r_3 = 1.44$. (d) A chaotic attractor results for the parameter value $r_3 = 1.291$, which is close to a boundary crisis.

As depicted in Fig. 2(a), for $r_3 = 1.65$, the additional (to M) attractor \mathcal{A} is regular and periodic. This attractor is a stable limit cycle. At the bifurcation point $r_3 = 1.573$, this 1-cycle loses its stability and is transformed into a stable 2-cycle. A further decrease of the recruitment produces a standard period-doubling cascade, and the attractor \mathcal{A} is transformed into the full chaotic strange attractor shown in Fig. 2(c).

Thus, the attractor \mathcal{A} represents a variety of stable dynamical coexistence of healthy, immune and tumor cells populations, with changing r_3 . The chaotic attractor disappears at the crisis bifurcation point $r_3^c = 1.2909$. The system behavior near this crisis bifurcation point was studied in detail in [López *et al.*, 2014a]. In the bifurcation diagram appearing in Fig. 3, the equilibrium $M(1, 0, 0)$ is shown by a black line (solid for stable and dashed for unstable), while a family of attractors \mathcal{A} shaping a Feigenbaum's tree is plotted in blue color. Here, x -coordinates of local maxima of attractors are shown. In summary, in the interval $1.25 \leq r_3 \leq 1.65$, one can distinguish three parametric zones, depending on the levels of T-cell recruitment:

- (1) A *dead* monostable zone ($1.25 \leq r_3 \leq r_3^c$): here, the equilibrium $M(1, 0, 0)$ is a single global attractor and the solutions of the deterministic system tend towards $M(1, 0, 0)$ asymptotically for any initial data. Therefore, in this range, the population of effector and healthy cells are out-competed by tumor cells independently of

the relative initial sizes of the cell populations. In other words, insufficient levels of recruitment permit the settlement of the tumor no matter what.

- (2) A *hazardous* bistable zone ($r_3^c \leq r_3 \leq r_3^*$): in this region, depending on the initial conditions, solutions of Eqs. (2) may tend either to $M(1, 0, 0)$ or to the oscillatory attractor \mathcal{A} (chaotic or periodic). In Fig. 3, the separatrix dividing basins of attraction of M and \mathcal{A} is shown by a red dashed line. There is here enough recruitment of effector cells so as to hinder the tumor growth, as long as the size of the latter is not too close to its carrying capacity.
- (3) A *safe* monostable zone ($r_3^* \leq r_3 \leq 1.65$): here, all solutions starting from the initial point with positive coordinates tend to the periodic attractor. In the narrow subinterval $1.56 < r_3 < 1.573$, this attractor is a 2-cycle, and in the subinterval $1.573 < r_3 < 1.65$ this attractor is a 1-cycle. The recruitment here is more than sufficient to keep the tumor below its carrying capacity, performing periodic oscillations in size.

Examples of oscillatory attractors are shown in Fig. 2 in blue color. In red color, phase trajectories leaning towards the equilibrium $M(1, 0, 0)$ are plotted. As can be seen in the bifurcation diagram appearing in Fig. 3, this system exhibits a plethora of bifurcations and dynamical regimes, both regular and chaotic. Furthermore, depending on the

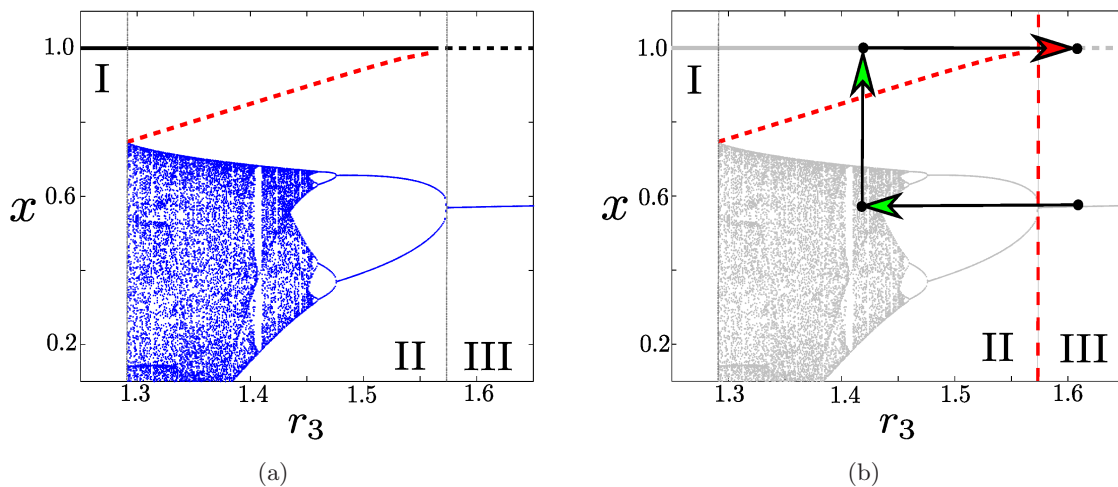


Fig. 3. *Bifurcation diagram of the deterministic system.* (a) The tumor size population is plotted against the parameter r_3 . The equilibrium $M(1, 0, 0)$ is plotted with a black line (solid for stable and dashed for unstable). The oscillatory attractor \mathcal{A} is plotted in blue. It loses stability and leads to chaotic behavior as the recruitment decreases through a period doubling cascade. The separatrix is shown in red. (b) A hysteresis loop showing how the fluctuations move along the bifurcation diagrams. Green arrows are allowed transitions, while the red arrow represents a forbidden transition.

parameter r_3 , monostable and bistable zones can be determined. It is well known that noise represents an inevitable attribute in the dynamics of cell biology that can crucially change the fate of the system. In the following lines, we examine how noise impacts the interactions of tumor, healthy and immune cells populations in mono and bistable zones. As we shall see, recruitment fluctuations can dramatically impair the establishment of the tumor.

3. Stochastic Model

Now we consider the behavior of the system of Eqs. (2) under random disturbances since the tumor growth does not usually take place in a deterministic manner. To simulate the effect of external fluctuations, we use the following system of stochastic differential equations in the Ito sense

$$\begin{aligned}\dot{x} &= x(1-x) - a_{12}yx - a_{13}zx \\ \dot{y} &= r_2y(1-y) - a_{21}xy \\ \dot{z} &= (r_3 + \varepsilon\xi(t))\frac{x}{x+k_3}z - a_{31}x - d_3.\end{aligned}\quad (3)$$

Here, the random forcing $\xi(t)$ is an uncorrelated white Gaussian noise term with parameters $\langle \xi(t) \rangle = 0$, $\langle \xi(t)\xi(\tau) \rangle = \delta(t-\tau)$, and ε represents the noise intensity. Since the model is dissipative, we can neglect small correlations in the noise. Moreover, because we are focusing our attention on the effect of fluctuations in T-cell recruitment, the noise term has been introduced in a multiplicative way by a perturbation of the recruitment parameter r_3 . We also recall that additive noise is inadequate in population models, since cell populations are restricted to take positive values. Consequently, we assume that the fluctuations in the immune cell populations are dominantly produced through the complex dynamical process of cell recruitment described in the introduction, which depend on multiple internal events, but also on events that are external to the tumor. This fact justifies the use of a Langevin approach [Van Kampen, 1992]. Note that the equilibrium $M(1, 0, 0)$ of the model appearing in Eqs. (2) is also the equilibrium of the stochastic model represented by Eqs. (3), because of the structure of the noisy term. Therefore, the solutions of the former starting from $M(1, 0, 0)$ never leave this point for any ε . This fact will be crucial to explain the dynamics of the system and will be

responsible for producing a previously undetected extinction effect.

We begin by analyzing the stochastic dynamics of the model appearing in Eqs. (3) in the *hazardous* bistable zone $r_3^c \leq r_3 \leq r_3^*$, since it is the most sensitive to noise of the two last parameter regions. Under time varying random disturbances, solutions can leave the deterministic oscillatory attractor \mathcal{A} . For weak noises, random trajectories are concentrated near the deterministic attractor. As noise increases, the dispersion of random trajectories increases as well. Now the random trajectory can cross the separatrix between basins of attraction of M and \mathcal{A} , to later on, approach the point M . The density x of tumor cells tends to one, and the healthy cell populations of the tissue y, z are led to extinction. Here, we observe a noise-induced transition from the regime of the coexistence of healthy, immune and tumor cells to the absolute tumor dominance. Importantly, this extinction of both cell compartments occurs in an irreversible fashion, since once the cytotoxic effector cells are eradicated, no more T-cells can be recruited. We insist that this occurs in our model because the recruitment process is based on a feedback mechanism relying on the existence of effector T-cells. The same holds for the healthy normal cells, which can only grow from other cells (the stem ones) of the same lineage.

The effect of a noise-induced extinction is frequently observed in biological systems [Sardanyés & Alarcón, 2018; Tsimring, 2014], and it is not surprising at all in multistable systems. Such stochastic transitions are numerically shown in Fig. 4 by inspection of the time series for different values of r_3 . As is immediately observed, the closer r_3 is to the crisis bifurcation point r_3^c , the smaller the size of the perturbations required to transfer the system from the oscillatory attractor \mathcal{A} to the equilibrium M . The dynamics of trajectories in phase space are shown in Fig. 5. More importantly, under the influence of noise, such noise-induced transitions can be observed from the monostable zone $r_3^* \leq r_3 \leq 1.65$, which was classified as *safe* in the deterministic system. Indeed, in this zone [see Fig. 2(d) for $r_3 = 1.6$], increasing the fluctuations results in the transition of the stochastic system to the equilibrium M . Note that in this zone the equilibrium M is unstable. Therefore, this phenomenon can be described mathematically as a noise-induced

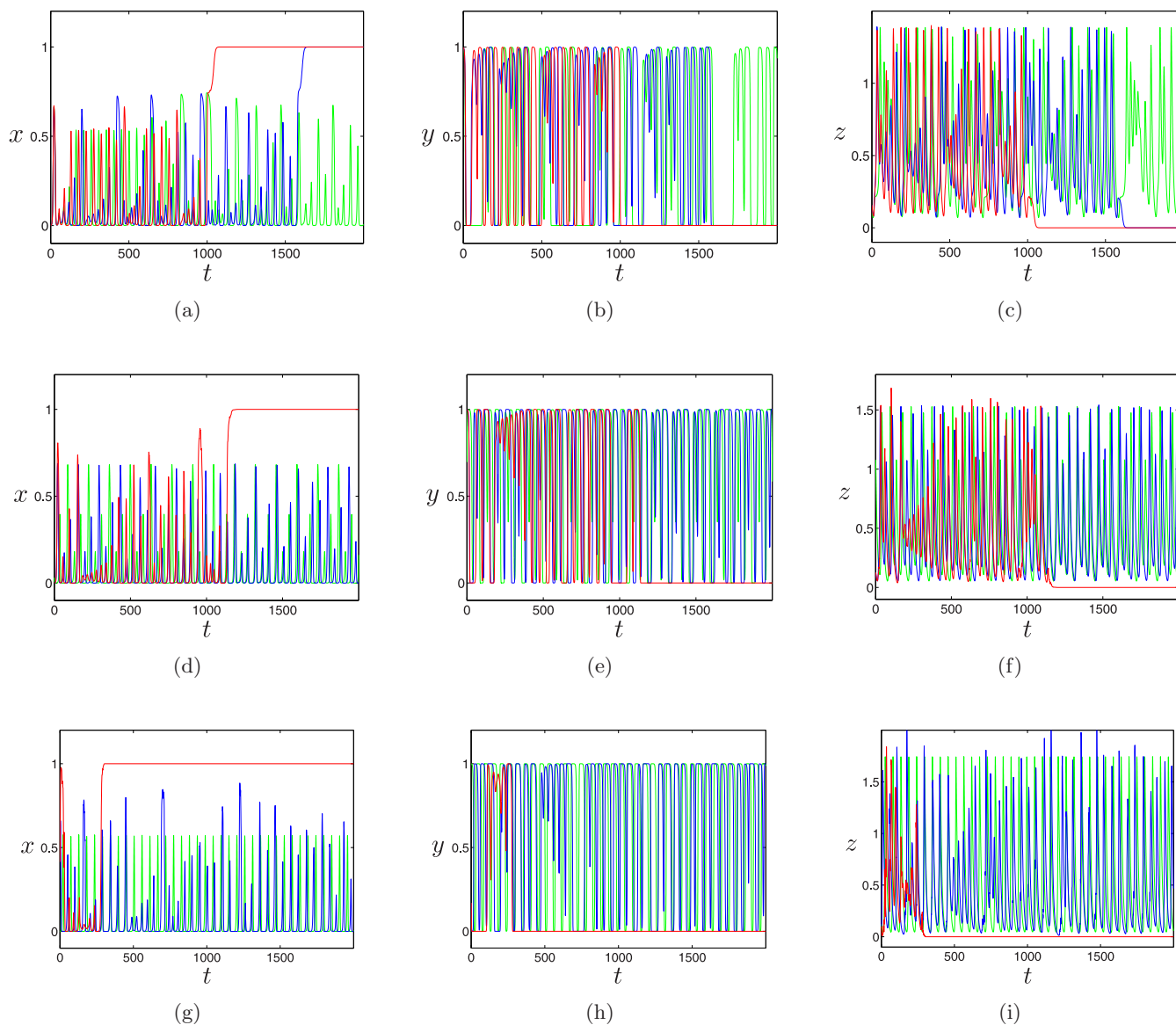


Fig. 4. Time series of the solutions of both the deterministic (green color) and the stochastic system (red and blue colors). (a)–(c) The evolution of tumor x , healthy y and immune cells z for a recruitment value of $r_3 = 1.291$ in the hazardous zone and noise intensities $\varepsilon = 0.01$ (blue) and $\varepsilon = 0.02$ (red). (d)–(f) A higher recruitment value in the same parameter region with $r_3 = 1.409$ and noise intensities $\varepsilon = 0.02$ (blue) and $\varepsilon = 0.2$ (red). (g)–(i) A recruitment value of $r_3 = 1.6$ and noise intensities $\varepsilon = 0.4$ (blue) and $\varepsilon = 0.8$ (red).

stabilization of the unstable equilibrium by parametric noise.

The process occurs through a hysteresis phenomenon which, as far as we know, it had not been previously reported in the literature on mathematical oncology and physics of cancer. It can be explained in the bifurcation diagram as shown in Fig. 3(b). In the first place, recruitment fluctuations permit an excursion from the *safe* region to the *hazardous* zone. This phenomenon produces an

instability of the tumor cell population trajectories, which are now allowed to perform chaotic oscillations, occupying a bigger portion of the phase space. But now, since the fluctuations in the cell recruitment are still present, a transition similar to the one described in the previous paragraph might occur. Then, since the fluctuations are not affecting anymore the extincted populations, they cannot drive back the tumor to small values. Collaterally, the healthy cells are also dragged to extinction and

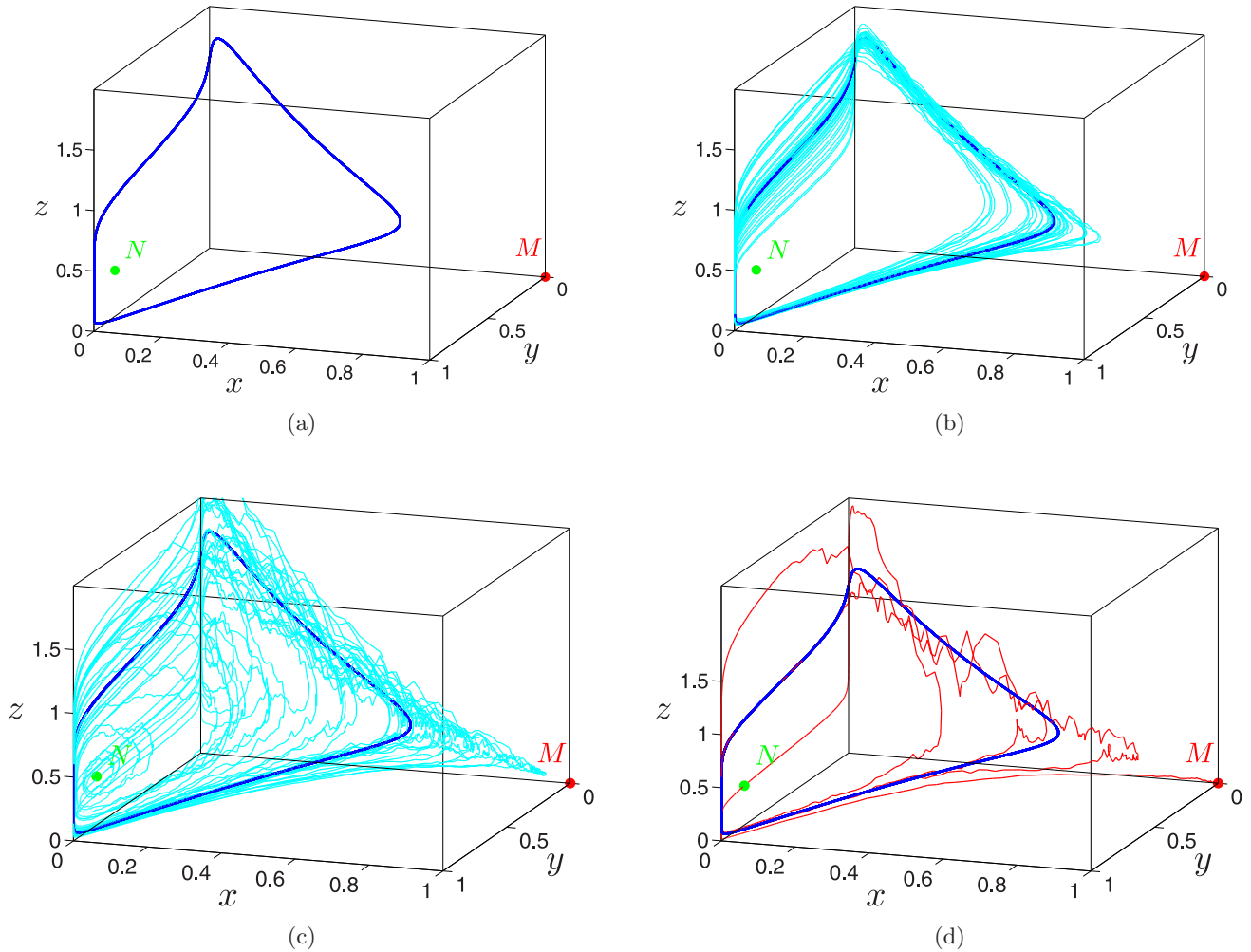


Fig. 5. *The effects of noise on phase space trajectories.* (a) The deterministic periodic cycle for $r_3 = 1.6$. (b) The same trajectory with a white multiplicative noise $\varepsilon = 0.1$, which is not sufficient to break the periodicity of the cycle. (c) The same situation with higher fluctuations given by $\varepsilon = 0.4$. Now the trajectories resemble the deterministic chaotic attractor previously shown, with fluctuations superimposed. However, the malignant attractor is not easily reached. (d) When the fluctuations are sufficiently intense ($\varepsilon = 0.8$), the tumor is rapidly stabilized.

the tumor is stabilized at its maximum value, making useless the efforts of the cell mediated immune response. This fact suggests that the process of recruitment in aggressively growing tumors might be very important concerning the effectiveness the immune response and the associated preservation of the healthy host tissue.

4. Noise-Induced and Chaos-Order Transitions

For the detailed study of such noise-induced transitions, we will use a parametric analysis of some statistics. First, we consider the mean values μ_x, μ_y , and μ_z of the coordinates of random solutions of system (3) during the time interval $[0, T]$. For example, the time average of the tumor cell population can

be written as

$$\mu_x = \frac{1}{L} \sum_{k=0}^L x(kh), \quad h = \frac{T}{L}.$$

Another important statistic is the size of the fluctuations, which can be estimated by means of the second cumulant, defined as

$$\sigma_x^2 = \frac{1}{L} \sum_{k=0}^L x^2(kh) - \mu_x^2, \quad h = \frac{T}{L}.$$

As an initial value of these solutions, we take the unstable nontrivial equilibrium N . A dependence of the mean values on the parameters r_3 and ε is shown in Fig. 6 for $h = 0.01$ and $T = 10^3$. As can be seen, under increasing noise intensity, the mean value μ_x of tumor cells monotonously increases and

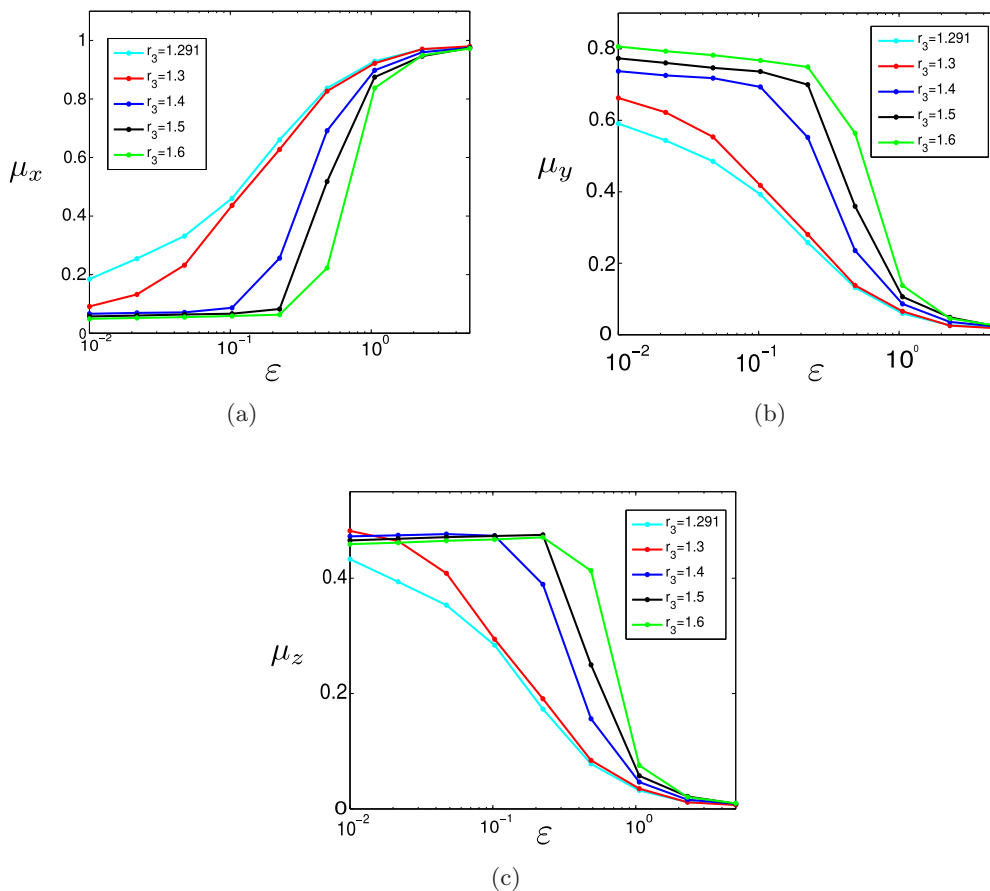


Fig. 6. The time-averaged values of the solutions of the stochastic system for the three cell populations. Here we are using an interval $[0, T]$ with $T = 1000$. (a) Average size of tumor cells. We see a transition from small tumor burdens to sizes close to the carrying capacity. This means that noise facilitates tumor stabilization. (b) Average size of healthy cells. (c) Average size of immune cells. The ε -interval where the transition takes place shrinks as r_3 increases. The pattern for normal and immune cells is complementary to tumor cells.

tends to $\mu_x = 1$, whereas the mean values μ_y of healthy cells and μ_z of immune cells tend to zero. This scenario is observed in the bistable zone (see $r_3 = 1.291, 1.3, 1.4$) and in the monostable zone ($r_3 = 1.6$) as well. Note that mean values sharply change in a rather narrow window (ε -interval), specially for high values of the recruitment. Therefore, we see that those situations in which the immune response is weaker, the transition due to fluctuations occurs more easily and progressively for increasing values of the fluctuations.

From a mathematical point of view, the previous events occur because the separatrix curve is closer to the chaotic attractor and this facilitates the transition as shown in Fig. 3. Therefore, the location and the width of this ε -interval depends strongly on r_3 . The higher the levels of T-cell recruitment are, the greater it is the noise required for a transition to the *dead* zone, and the more sudden is the appearance of this transition.

Note that the green curves reflect a variation of mean values for $r_3 = 1.6$, which belong to the *safe* zone. As one can see, the deterministic instability of the *dead* equilibrium M does not guarantee a survival of healthy cells in the presence of noise if perturbations are present. This fact can be interpreted as a noise-induced extension of the dangerous zone. In Fig. 7 the previous conclusion is confirmed by studying the mean values of μ_x as a function of r_3 for the random solutions starting from the point N for different noise intensities ε and observation times T . Here, the extremum values of the x -coordinates of the attractor \mathcal{A} of the deterministic system of Eqs. (2) are also shown in grey. In this figure, one can compare how the mean values μ_x depend on r_3 for the two values $T = 10^3$ and $T = 10^4$.

Along with the mean values, the time averaged size of the fluctuations of each cell population has been computed and it is depicted in Fig. 8. For the

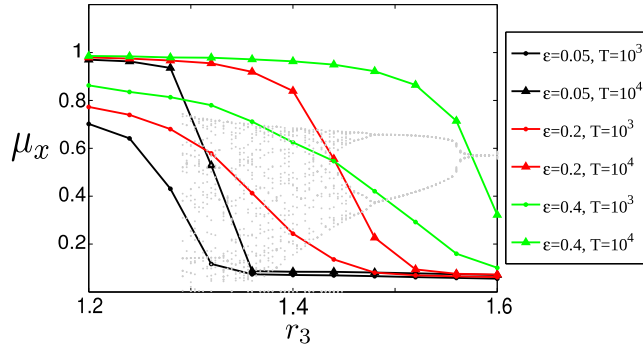


Fig. 7. Mean values μ_x of the solutions of the stochastic system against the recruitment of T-cells. Two time intervals $T = 10^3$ (circles) and $T = 10^4$ (triangles) are considered, and three different noise intensities $\varepsilon = (0.05, 0.2, 0.4)$, using different colors. A dependence on time average is detected. The longer the time interval, the sharper the transition from tumor stabilization to tumor contention. This suggests that, if we let T approach to infinity, in most situations we obtain a binary dynamical situation under the effects of noise. The bifurcation diagram is shown in the back in light gray to better correlate the dynamics and the mean values.

tumor cell populations the size of the fluctuations σ_x are peaked at intermediate values of the sigmoid curves described. Certainly, this occurs because the fluctuations are higher between the two limiting situations. The former corresponds to a tumor cell population that is retained at a stable small burden by the immune cells, and the other represents the opposite case, in which tumor dominates the struggle. Exactly the same occurs for the fluctuations of the other cell populations, since they are always in a relation of dependence. For the sake of completeness, we have also shown how the probability densities evolve as times goes by. This study is tantamount to deriving the Fokker–Planck equations, but computationally it is much more affordable. As can be seen in Fig. 9, an initial delta-peaked distribution of the tumor size localized at point N , evolves in time by splitting into two peaks. Then, this bimodal transient distribution evolves back into a sharp unimodal distribution centered at $x = 1$.

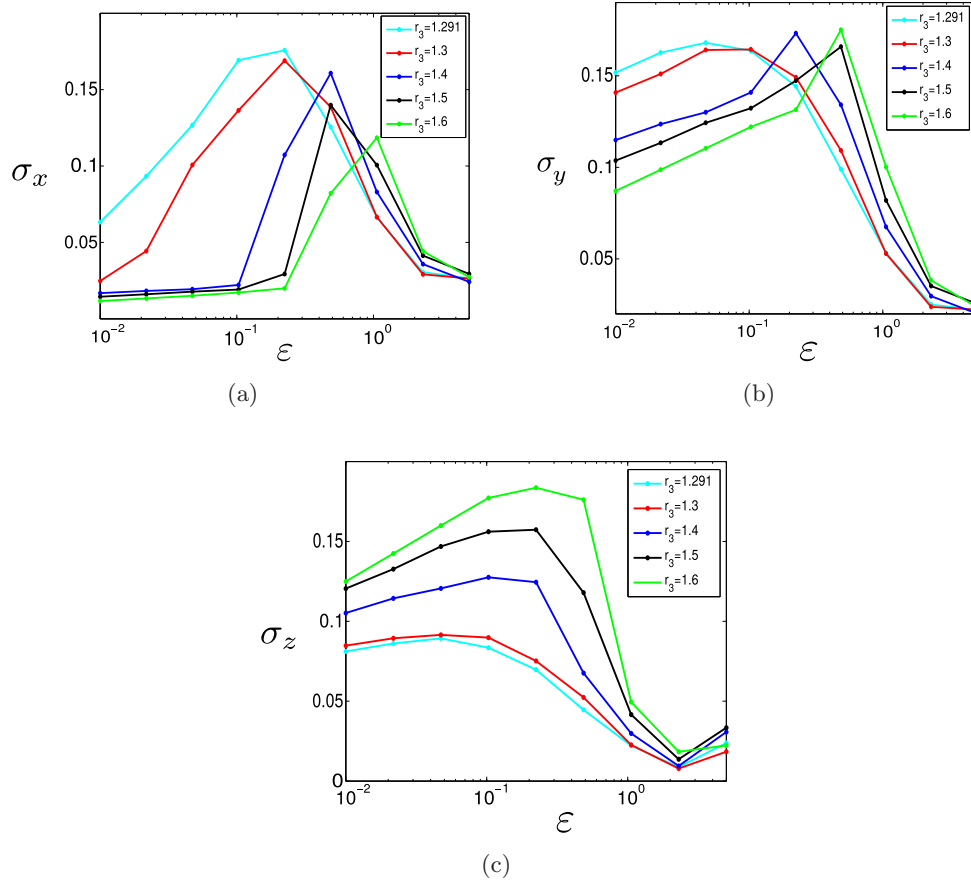


Fig. 8. Time averaged values for the mean squared deviation of the size of the three cell populations. Again, we are using an interval $[0, T]$ with $T = 1000$. The fluctuations peak around values for which the mean values of the cell populations take intermediate values. In other words, for medium noise intensities we see the most fluctuating cell populations, and we have more uncertainty on the asymptotic state of the system.

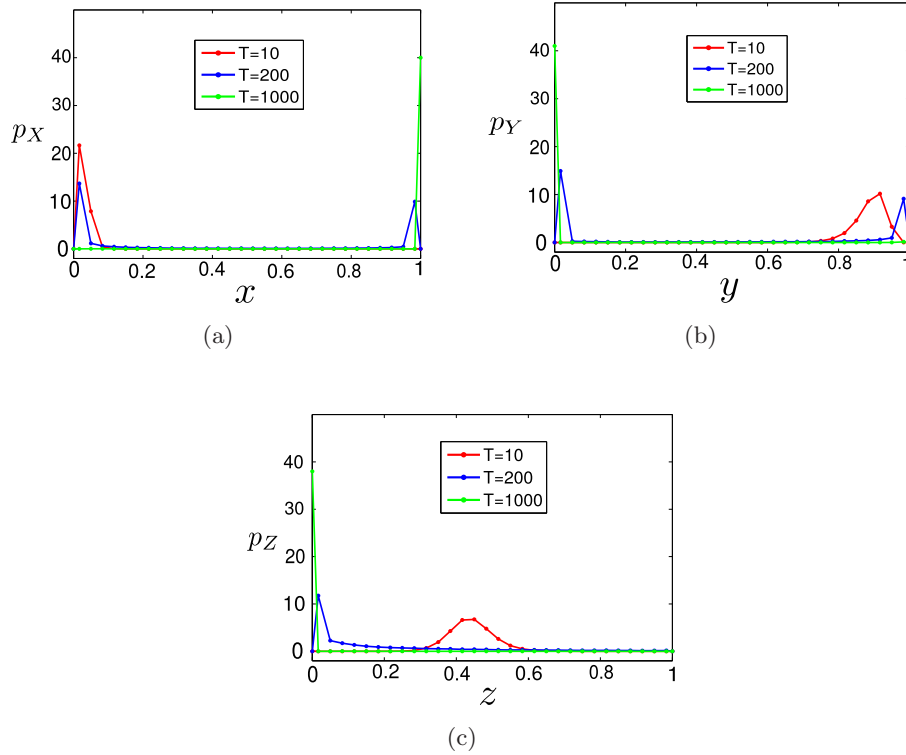


Fig. 9. Evolution of marginal probability density of each cell population with time. (a) The probability density $p_X(x)$ of tumor cells at three time instants T . The probability distribution, initially placed at the fixed point N , starts to diffuse and later on splits into two. Finally it concentrates at the malignant attractor M . (b) The probability density of healthy cells $p_Y(y)$ at three time instants T . The evolution is opposed to the evolution of the tumor cells, but dynamically similar. (c) The immune cell's probability density $p_Z(z)$ rapidly diffuses and drifts towards a delta-peaked distribution representing extinction.

Exactly the same process is observed for the normal cells, but with opposite fate. For the immune cells, however, the distribution directly evolves towards a sharp peak at zero.

We now proceed to characterize the probability of the transition of the stochastic model from the stable oscillatory regime of coexistence of tumor, healthy, and immune cells, to the *dead zone*. To describe probabilistically such transition, we need to introduce some formalization. Here, we assume that this system falls into the *dead zone* when $x(t)$ becomes close to one. Let δ be a parameter representing the proximity to one, then we define the region M_δ for which $x \geq \tilde{x} = 1 - \delta$ as a threshold value for x -coordinates of random solutions. In our calculations, we take $\delta = 0.01$. This means that the stochastic differential equation appearing in Eqs. (3) falls into the *dead zone* when $x(t) > \tilde{x} = 0.99$. Under this assumption, there exists a conditioned probability $p(M_\delta|N)$ of the transition of the stochastic system with the noise intensity ε to the *dead zone* during the fixed time interval $[0, T]$, when the system is originally very close to point N . This

magnitude represents the probability of the event $x(t) > 0.99$ for $0 \leq t \leq T$ with initial conditions as given.

In Fig. 10, a color map of $p(M_\delta|N)$ is plotted in the parameter space (r_3, ε) , with a fixed value $\delta = 0.01$. As can be seen, this function sharply increases in a very narrow ε -interval. A location of this ε -interval defines a threshold noise intensity corresponding to the transition to M . It should be noted that the $p(M_\delta|N)$ increases rather abruptly as r_3 increases. However, the location of this transition as a function of r_3 follows a nonlinear relation.

To conclude our investigation, we consider how the noise-induced transitions from the regime of the coexistence of healthy, immune, and tumor cells to the tumor dominance are accompanied by a chaos-order transformation. In Fig. 11, a dependence of the largest Lyapunov exponents Λ on the noise intensity ε is shown for various r_3 from the *hazardous zone*. Here, for $r_3 = 1.3$ and $r_3 = 1.4$, the deterministic attractor \mathcal{A} is chaotic, and for $r_3 = 1.5$ is regular (2-cycle). A change of the sign of Λ from plus to minus marks the transition from

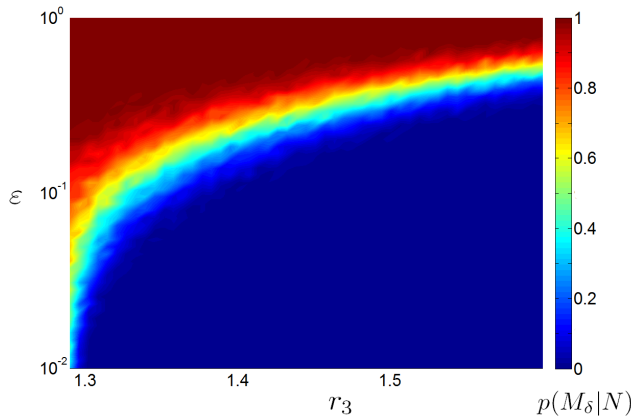


Fig. 10. The probability of exit towards the dead zone. The dead zone is defined as $M_\delta = \{x : x > 1 - \delta\}$, with $\delta = 0.01$ for the stochastic system conditioned to N , as a starting point. The color bar represents the probability of that event. As can be appreciated, a narrow ε -interval is observed for the transition to take place. Importantly, this window of transition describes a nonlinear curve as r_3 is varied.

chaos to order. As one can see, for r_3 close to r_3^c (see green curve for $r_3 = 1.3$), this transformation is observed for small noise intensities. For $r_3 = 1.4$ (see blue curve), this transformation from chaos to order occurs for a larger noise intensity.

If we calculate Λ for r_3 where regular oscillations are observed, then the scenario of these transformations changes. Indeed, for regular limit cycles, the largest Lyapunov exponent for $\varepsilon = 0$ equals

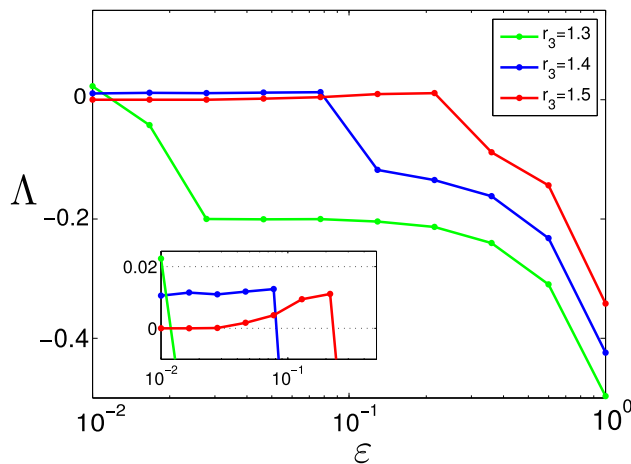


Fig. 11. The largest Lyapunov exponent plotted against the intensity of the fluctuations. For most values of r_3 a chaos to order transition is observed as fluctuations increase. However, for a value corresponding to periodic regions close to the period doubling bifurcation, a new phenomenon is observed. In the beginning we have regular dynamics, then the noise produces chaos, and finally the tumor is stabilized. The inset shows a magnification of the region where the Lyapunov exponent grows with the size of the fluctuations.

zero. Upon increasing the noise intensity, at first Λ increases and becomes positive (see red curve for $r_3 = 1.5$). With a further increase of ε , the largest Lyapunov exponent begins to decrease and becomes negative. So, here we have detected “order-chaos-order” transitions, which are induced by noise changes.

5. Conclusions and Discussion

We have studied the influence of parametric random fluctuations of T-cell recruitment in a known deterministic 3D cancer model. For parameter values representing aggressively growing tumors that are considerably immunogenic, three subintervals with qualitatively different dynamics were determined. The borders of these zones are defined by the crisis bifurcation of the chaotic attractor \mathcal{A} and the loss of the stability of the equilibrium M . To study stochastic effects, we considered a forced variant of the system with random fluctuations of the parameter r_3 . By direct numerical simulation of the time series, it was shown that in this system noise-induced transitions to the *dead zone* occur in a wide range of the parameter values of r_3 .

An important finding of the present work is that fluctuations in the recruitment of T-cells can drive a healthy host tissue to extinction and produce complete tumor dominance. We believe that this effect is interesting from a more general ecological point of view, since we are using a competitive Lotka–Volterra based model. The key point is as follows. Consider that two competing species are in a situation of imbalance, in such a manner that, in the absence of any other species, the dominant tends to produce the extinction of the weaker. Now, assume that an equilibrium among the two is kept by a third assistant species that provides balance by the destruction of the dominant individuals, leading to chaotic dynamics and bistability. Then, fluctuations which in principle only affect the size of the assistant species can be amplified by chaotic dynamics and lead to the extinction of the weakest individuals. Even if chaos is not at play, as we have shown, this extinction can be induced by the fluctuations themselves, as long as the fluctuations are sufficiently intense. In this manner, the dependence of the weak species on the assistant species becomes very strong, to the point that their fitness is mostly surrogated to their collaborators.

Concerning cancer therapy, the present research sheds light into the importance of the phenomenon

of T-cell recruitment. Even though a particular immunotherapy (e.g. CTLA-4 activity modulation by means of monoclonal antibodies [Ribas *et al.*, 2005], or the blocking of the PD-1 receptor) might lead to a substantial destruction of a tumor by the activation of T-cells, high levels of recruitment over a sustained period of time might be required to obtain the desired tumor remission. Otherwise, fluctuations in T-cell numbers could lead to undesired and unexpected effects, as shown in the present work. To conclude, it is important to note that the effect of fluctuations on tumor and healthy cell populations has been disregarded in the present model. Noise is permanently present in the growth of a tumor through pH variations, temperature, growth factors fluctuations, vascular evolution, etc. [Hanahan & Weinberg, 2011; Weinberg, 2013]. Therefore, further research is deserved to acquire a more complete view of the effect of random perturbations in tumor-immune interactions. In particular, we remark those concerning the intervention of other immune cell lineages and the role of the humoral immune response as well.

Acknowledgments

The work of Á. G. López, J. M. Seoane, M. A. F. Sanjuán on the study of deterministic dynamics was supported by the Spanish Ministry of Economy and Competitiveness and by the Spanish State Research Agency (AEI) and the European Regional Development Fund (ERDF) under Project No. FIS2016-76883-P. The work of I. Bashkirtseva and L. Ryashko on the study of stochastic dynamics was supported by the Russian Science Foundation (project 16-11-10098).

References

- Aguirre-Ghiso, J. A. [2007] “Models, mechanisms and clinical evidence for cancer dormancy,” *Nat. Rev. Cancer* **7**, 834–846.
- Anishchenko, V. S., Astakhov, V. V., Neiman, A. B., Vadivasova, T. E. & Schimansky-Geier, L. [2007] *Nonlinear Dynamics of Chaotic and Stochastic Systems. Tutorial and Modern Development* (Springer, Berlin).
- Bashkirtseva, I., Nasyrova, V. & Ryashko, L. [2018] “Analysis of noise effects in a map-based neuron model with Canard-type quasiperiodic oscillations,” *Commun. Nonlin. Sci. Numer. Simulat.* **63**, 261–270.
- Bellomo, N. & Preziosi, L. [2000] “Modelling and mathematical problems related to tumor evolution and its interaction with the immune system,” *Math. Comput. Model.* **32**, 413–452.
- Bellomo, N., Li, N. K. & Maini, P. K. [2008] “On the foundations of cancer modelling: Selected topics, speculations, and perspectives,” *Math. Models Methods Appl. Sci.* **18**, 593–646.
- Caravagna, G., d’Onofrio, A., Milazzo, P. & Barbuti, R. [2010] “Tumour suppression by immune system through stochastic oscillations,” *J. Theoret. Biol.* **265**, 336–345.
- De Pillis, L. G. & Radunskaya, A. [2003] “The dynamics of an optimally controlled tumor model: A case study,” *Math. Comput. Model.* **37**, 1221–1244.
- De Pillis, L. G., Radunskaya, A. E. & Wiseman, C. L. [2005] “A validated mathematical model of cell-mediated immune response to tumor growth,” *Cancer Res.* **65**, 235–252.
- De Pillis, L. G., Gu, W. & Radunskaya, A. E. [2006] “Mixed immunotherapy and chemotherapy of tumors: Modelling, applications and biological interpretations,” *J. Theor. Biol.* **238**, 841–862.
- Dunn, G. P., Old, L. J. & Schreiber, R. D. [2004] “The three Es of cancer immunoediting,” *Annu. Rev. Immunol.* **22**, 329–360.
- Fiasconaro, A., Spagnolo, B., Ochab-Marcinek, A. & Gudowska-Nowak, E. [2006] “Co-occurrence of resonant activation and noise-enhanced stability in a model of cancer growth in the presence of immune response,” *Phys. Rev. E* **74**, 041904.
- Gao, J. B., Hwang, S.K. & Liu, J. M. [1999] “When can noise induce chaos?” *Phys. Rev. Lett.* **82**, 1132–1135.
- Hanahan, D. & Weinberg, R. A. [2011] “Hallmarks of cancer: The next generation,” *Cell* **144**, 646–673.
- Horsthemke, W. & Lefever, R. [1984] *Noise-Induced Transitions* (Springer, Berlin).
- Itik, M. & Banks, S. [2010] “Chaos in a three-dimensional cancer model,” *Int. J. Bifurcation and Chaos* **20**, 71–79.
- Janeway, C. A., Travers, P., Walport, M. & Shlomchik, M. J. [2012] *Immunobiology* (Garland Science, NY).
- Kuznetsov, V. A., Makalkin, I. A., Taylor, M. A. & Perelson, A. S. [1994] “Nonlinear dynamics of immunogenic tumors: Parameter estimation and global bifurcation analysis,” *Bull. Math. Biol.* **56**, 295–321.
- Lasinska, I., Kolenda, T., Teresiak, A., Lamperska, K. M., Galus, L. & Mackiewicz, J. [2019] “Immunotherapy in patients with recurrent and metastatic squamous cell carcinoma of the head and neck,” *Anti-cancer Agents Med. Chem.* **19**, 290–303.
- Li, D. X. & Zhao, Y. [2019] “Survival analysis for tumor cells in stochastic switching environment,” *Appl. Math. Comp.* **357**, 199–205.
- Lindner, B., Garcia-Ojalvo, J., Neiman, A. & Schimansky-Geier, L. [2004] “Effects of noise in excitable systems,” *Phys. Rep.* **392**, 321–424.

- Liu, X., Li, Q. & Pan, J. [2018] “A deterministic and stochastic model for the system dynamics of Tumor–Immune responses to chemotherapy,” *Physica A* **500**, 162–176.
- López, Á. G., Sabuco, J., Seoane, J. M., Duarte, J., Januário, C. & Sanjuán, M. A. F. [2014a] “Avoiding healthy cells extinction in a cancer model,” *J. Theor. Biol.* **349**, 74–81.
- López, A. G., Seoane, J. M. & Sanjuán, M. A. F. [2014b] “A validated mathematical model of tumor growth including tumor–host interaction, cell-mediated immune response and chemotherapy,” *Bull. Math. Biol.* **76**, 2884–2906.
- López, A. G., Seoane, J. M. & Sanjuán, M. A. F. [2017a] “Bifurcation analysis and nonlinear decay of a tumor in the presence of an immune response,” *Int. J. Bifurcation and Chaos* **27**, 1750223.
- López, A. G., Seoane, J. M. & Sanjuán, M. A. F. [2017b] “Dynamics of the cell-mediated immune response to tumour growth,” *Phil. Trans. R. Soc. A* **375**, 20160291.
- McDonnell, M. D., Stocks, N. G., Pearce, C. E. M. & Abbott, D. [2008] *Stochastic Resonance: From Suprathreshold Stochastic Resonance to Stochastic Signal Quantization* (Cambridge University Press, Cambridge).
- Miller, M. J., Wei, S. H., Cahalan, M. D. & Parker, I. [2003] “Autonomous T cell trafficking examined in vivo with intravital two-photon microscopy,” *Proc. Natl. Acad. Sci. USA* **100**, 2604–2609.
- Nani, F. & Freedman, H. I. [2000] “A mathematical model of cancer treatment by immunotherapy,” *Math. Biosci.* **163**, 159–199.
- Ribas, A., Camacho, L. H., Lopez-Berestein, G., Pavlov, D., Bulanhagui, C. A., Millham, R. et al. [2005] “Antitumor activity in melanoma and anti-self responses in a phase trial with the anti-cytotoxic T lymphocyte-associated antigen 4 monoclonal antibody CP-675,206,” *J. Clin. Oncol.* **23**, 8968–8977.
- Ryashko, L. B. & Slepukhina, E. S. [2017] “Noise-induced torus bursting in the stochastic Hindmarsh–Rose neuron model,” *Phys. Rev. E* **96**, 032212.
- Sardanyés, J. & Alarcón, T. [2018] “Noise-induced bistability in the fate of cancer phenotypic quasispecies: A bit-strings approach,” *Sci. Rep.* **8**, 1027.
- Teng, M. W. L., Swann, J. B., Kohebel, C. M., Schreiber, R. D. & Smyth, M. J. [2008] “Immune-mediated dormancy: An equilibrium with cancer,” *J. Leukoc. Biol.* **18**, 645–653.
- Tsimring, L. S. [2014] “Noise in biology,” *Rep. Progr. Phys.* **77**, 026601.
- Van Kampen, N. G. [1992] *Stochastic Processes in Physics and Chemistry* (Elsevier, The Netherlands).
- Weinberg, R. A. [2013] *The Biology of Cancer* (Garland Science, NY).
- Wodarz, D., & Komarova, N. L [2014] *Dynamics of Cancer: Mathematical Foundations of Oncology* (World Scientific Publishing, Singapore).
- Yang, J., Tan, Y. S. & Cheke, R. A. [2019] “Thresholds for extinction and proliferation in a stochastic Tumour–Immune model with pulsed comprehensive therapy,” *Commun. Nonlin. Sci. Numer. Simulat.* **73**, 363–378.